


## Article

# Local Frequency Modulation Strategy Based on Controllable Load Characteristic Identification of Multi-Port Power Router

Changhao Lv \*, Qingquan Jia, Lijuan Lin  and Jinwei Cui

Key Lab of Power Electronics for Energy Conservation and Motor Drive of Hebei Province, Yanshan University, Qinhuangdao 066004, China

\* Correspondence: codedanny@163.com

**Abstract:** The scarcity of inertial resources in the new AC–DC hybrid grids makes the grid frequency prone to fluctuation. In this paper, the relationship between the grid-side and load-side characteristics of the power router is constructed. By adjusting the port load parameters, the load power can respond quickly to the fluctuation of the grid frequency, thereby realizing rapid support of the grid frequency. Firstly, two kinds of mathematical models for sensitivity identification of load characteristics, variable voltage and variable frequency, are established to calculate the characteristic parameters of a multi-port load. The allocation rules of port power and allocation coefficients are designed according to the parameters. A frequency modulation control method that matches the load response capability of the multi-port router is proposed. Then, taking into consideration the uncertainty of load group characteristics and power, a variable coefficient frequency modulation control strategy for a multi-port power router that can adapt to the adjustable margin of loads is proposed. The proposed model is built based on a Simulink platform for validation. The simulation results show that the proposed frequency modulation strategy can be added, and the frequency modulation performance of the power grid is further improved compared to the situation without this method. The frequency is suppressed to 49.93 HZ. It is verified that this method can make the controllable load respond sensitively and effectively to grid disturbance.

**Keywords:** hybrid grid; controllable load; characteristic identification; fast frequency modulation; variable coefficient control; local control



**Citation:** Lv, C.; Jia, Q.; Lin, L.; Cui, J. Local Frequency Modulation Strategy Based on Controllable Load Characteristic Identification of Multi-Port Power Router. *Energies* **2023**, *16*, 3651. <https://doi.org/10.3390/en16093651>

Academic Editor: David Macii

Received: 31 March 2023

Revised: 19 April 2023

Accepted: 20 April 2023

Published: 24 April 2023



**Copyright:** © 2023 by the authors. Licensee MDPI, Basel, Switzerland. This article is an open access article distributed under the terms and conditions of the Creative Commons Attribution (CC BY) license (<https://creativecommons.org/licenses/by/4.0/>).

## 1. Introduction

With the continuous improvement of new energy penetration rate in power systems, the proportion of traditional generating units gradually decreases and the inertia resources in the power grid become increasingly scarce. In the new AC–DC interconnected power grids, due to the increase in resource types for frequency modulation, the distribution of resources is becoming more dispersed, resulting in the weakening of spatiotemporal coupling of the overall grid frequency. At the same time, the uncertainty and time variability brought by the new energy sources gradually worsen, which essentially leads to the decline of overall inertial support and the anti-interference abilities of the power grid. Owing to these reasons, the frequency stability of these power systems also face severe challenges [1].

At present, the “source grid load” system has changed from having the traditional single supply-and-demand relationship to having more advanced multi-energy coordination and interaction forms. The means of control and frequency modulation of the grid are also more diverse. The feasibility of smart grid construction based on a controllable power router has been researched [2]. It has been shown that a power router can connect the AC and DC systems, integrate the new energy into grid, and realize efficient power flow management and frequency modulation control. Meanwhile, existing papers have performed a lot of research on frequency modulation methods for different resources in power systems, for example: traditional generator frequency modulation control at the source end and

droop control frequency modulation mode of distributed power generation [3–5], as well as energy storage technology that can be controlled at the “source grid load” end [6,7]. A self-frequency recovery control method using an interval type-2 fuzzy integrator controller has also been proposed [8]. More specifically, a central controller and a local controller were set in the paper; the local controller directly implemented frequency regulation of the distributed power supply. A centralized frequency control method has been adopted and a grid inverter control strategy using a virtual synchronous machine was proposed in [9]. The above articles researched different frequency-regulation objects. For energy storage equipment, on one hand, there is a shortage of capacity for participating in grid frequency modulation. On the other hand, large-scale energy storage has a high cost. It is difficult to achieve a satisfactory frequency modulation effect. Moreover, these frequency modulation methods all require large-scale communication as the premise, and there is still the problem of response lag. There is a lack of means and measures to respond quickly to frequency regulation in response to the random fluctuations caused by new energy and other factors [10]. Therefore, new frequency modulation methods are urgently needed to meet the system’s need for suppressing frequency disturbances.

As an important carrier of demand-side response, power load has great potential for regulation and control [11]. Likewise, many studies have been reported on load aggregation management, forecast planning and operation optimization, and so on [12–14]. However, in terms of frequency regulation, due to the wide variety of loads, complex characteristics, and difficult management and control [15], accurately modeling and controlling the load so that it can quickly participate in power grid frequency regulation is still a problem that needs to be studied in depth [16]. The precondition for controlling the autonomous response of loads to grid frequencies is to obtain the load status and basic characteristic parameters. The load sensitivity identification method can obtain a characteristic model of the load by sampling some parameters of the actual load. A sensitivity identification method for an intelligent transformer has been proposed [17]. This method can realize real-time measurement and does not affect power quality. This research only studies the theoretical method of load identification, and does not further study the applicable scenarios.

In terms of the control and optimization of the load participation frequency, the literature [18] uses the given load variation, and by combining it with the generator operating characteristics, it judges the load sensitivity and performs load-shedding control when the power grid is at low frequency. An adaptive load frequency control method is proposed in [19]. This method takes into account nonlinear factors such as frequency threshold and time delay and applies a new continuous low-frequency load shedding scheme according to traditional method. A strategy of under-frequency load shedding involving UHVDC is proposed in [20]. The frequency regulation characteristics of new energy after grid connection is analyzed, and the frequency response model is established. Although identification technology is applied to the frequency modulation method in [18], the frequency modulation method of load shedding can easily cause a certain impact on the power grid [21]. Moreover, the above methods only study specific scenarios, such as the load control when the grid frequency is reduced, and do not give a complete solution to a sudden increase in grid frequency. Reference [22] utilizes intelligent load technology for primary frequency regulation and proposes an improved optimal load control method. However, this method needs to solve the parameter calculation in scheduling and the response speed is slow, which makes it difficult to meet real-time needs. In [23], the optimal frequency scheme of grid load considering constant delay and time-varying delay is studied and designed for the time-delay problem caused by communication. A frequency regulation controller based on an intelligent transformer is presented in [24]. The controller adjusts the load power by controlling the load terminal voltage in order to realize a real-time response to grid frequency changes. However, this research only considers the voltage parameters, and the load frequency modulation mean is single. A control algorithm using virtual inertia technology to effectively suppress the frequency oscillation of the system is proposed when the load changes by controlling the charging of electric vehicles in [25]. In [26], a two-level

control model of cluster temperature control load is proposed. The upper layer coordinates the response of multiple aggregators using centralized control commands, and the lower layer implements distributed control of air-conditioning clusters.

In conclusion, optimal control of traditional primary frequency modulation as well as medium and long time scales have been researched in some literature. However, these frequency modulation methods do not solve the problems caused by weak inertia in the new power grids; their inherent frequency modulation characteristics lead to response delays, and the response time reaches more than second level. Some studies have conducted discussions on frequency modulation control for systems with centralized and distributed structures. However, no matter what kind of structure it is, the upper-layer system needs to issue instructions uniformly to implement control, and there will inevitably be a lot of communication in the system. There are also some works on the frequency modulation of specific types of loads, but the frequency modulation methods are single and the frequency modulation potential of the large amount of load in the power grid is not tapped and used. Moreover, these studies overlook problems such as load response lag, so the frequency modulation effect has great limitations. The new power systems have higher requirements for fast and stable frequency modulation. With the lack of grid inertia and the increased uncertainty and randomness of disturbances, the frequency problem caused by grid shocks becomes more and more serious. The response delay caused by the large amount of communication and other factors, as well as the lack of frequency modulation means, make it difficult for the above frequency modulation method to support the frequency of a power grid quickly and effectively.

Aiming at the above problems, a local frequency control method based on a multi-port load characteristic identification of a power router is proposed. This method does not need a large amount of centralized communication, and by embedding the frequency regulation control method into the local controller, an autonomous response to port load can be realized so as to support the frequency of the power grid quickly and effectively, which alleviates the problem of the lack of grid inertia and fully improves the load utilization rate and gives play to frequency modulation potential.

1. Firstly, obtaining the real-time status of the load lays the foundation for fast frequency control. The mathematical sensitivity models of the two types of load characteristics are established, and the characteristic parameters of the multi-port load are calculated according to the identification results. This parameter can effectively evaluate the adjustment capability of the port load and serve as the basis for port power allocation. On this basis, the characteristics of multi-port load groups are divided into variable voltage and variable frequency, which can control their orderly participation in grid frequency modulation.
2. Then, the frequency regulation characteristics of the controllable load that can respond to the frequency demand of the grid are established, and a fast frequency regulation control method for multi-port loads is proposed. By detecting the frequency feedback at the grid end, autonomous controllable load frequency modulation response can be achieved. This method can be flexibly applied to the AC and DC ports of power routers. The variable voltage and variable frequency control corresponding to load characteristics is implemented for different port load groups.
3. A variable-parameter frequency regulation control strategy that can adapt to the load state is proposed. This strategy takes into account the uncertainty of load groups' power between cycles, divides the load response frequency interval, and makes full use of the adjustable load allowance. Smooth frequency modulation is realized on an adjustable frequency segment. This strategy can realize rapid frequency modulation of the controllable load to the power grid at the initial disturbance stage, obtain the response time for other frequency modulation means such as new energy frequency modulation and primary frequency modulation, and improve the overall frequency modulation capability of the power grid. Finally, a controllable load frequency modu-

lation control model based on the Simulink platform is built and used for verifying the effectiveness of the proposed method.

## 2. Basic Architecture and Scheme of Multi-Port Load Frequency Modulation

A power router has the characteristics of strong flexibility and controllability, and can provide topology ports with different functions according to need. It is widely applied in the new power systems. Moreover, its power load is large in size and rich in resource potential. Without affecting the normal power supply, if the fast fine-tuning of the voltage and frequency of the load group is implemented through the port control of the power router so that load power can follow the change in grid frequency in real time, the frequency disturbance can be effectively suppressed and the frequency problem caused by the insufficient inertia of new power systems can be solved.

### 2.1. Load Control Topology of The Multi-Port Power Router

The proposed multi-port controllable load frequency modulation control strategy takes the power router as its basic structure. The basic structure of a power router has at least the following types of ports: AC grid-connected port, AC load port with variable voltage and variable frequency control, and DC load port. The basic topology of a power router is shown in Figure 1.

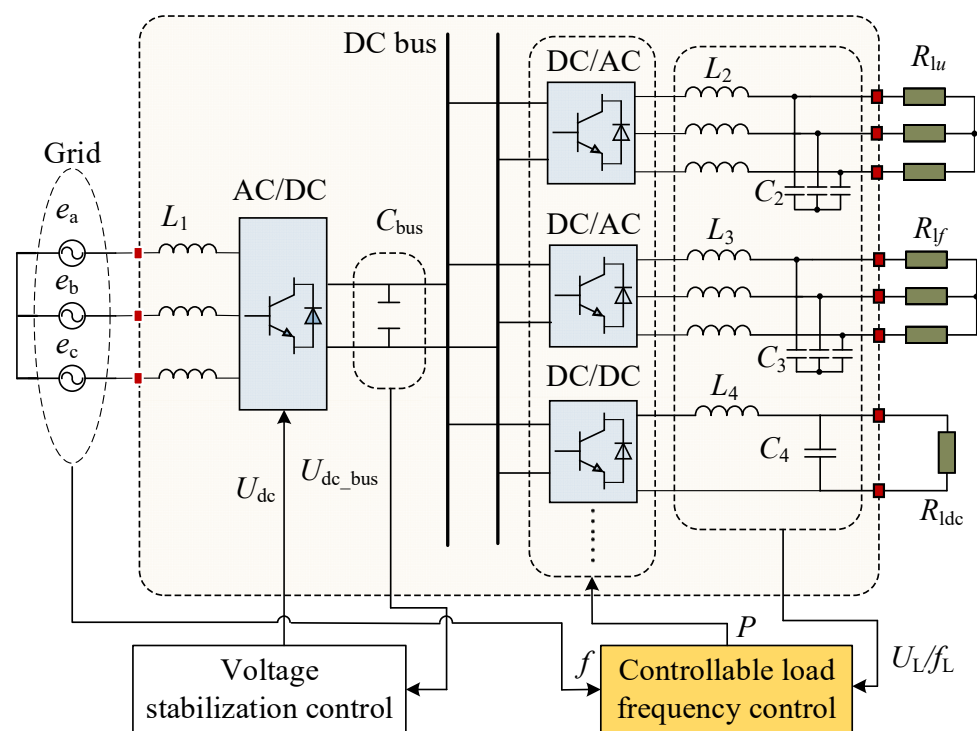


**Figure 1.** Schematic diagram of multi-port power router topological structure.

In Figure 1,  $L_1$  is the net-side filter inductance;  $L_2$ ,  $L_3$ ,  $C_2$ , and  $C_3$  are the AC output port filter inductances and capacitances, respectively;  $L_4$  and  $C_4$  are the filter inductance and capacitance of the DC load port, respectively;  $C_{bus}$  is the DC bus capacitance;  $U_{dc}$  is the command value of the DC bus voltage;  $R_{lu}$ ,  $R_{lf}$ , and  $R_{ldc}$  are the AC voltage-sensitive load, frequency-sensitive load, and DC variable voltage load, respectively.

In Figure 1, an AC/DC grid-connected port is used to connect to the power grid; the main function of the rectifier and voltage regulator control is to stabilize the DC bus voltage and achieve rapid power transfer. DC/AC and DC/DC output ports are used for controllable load group access. Each group of load ports has variable voltage and variable frequency functions. Through the controllable load frequency control method, the load port power output can respond according to the needs of the grid frequency. When the

grid frequency changes due to interference, the load port of the power router can adjust the output power command value according to the frequency modulation characteristic and further change the voltage amplitude or frequency of the load port. By controlling the increase or decrease in the load power, the disturbance in the power grid is suppressed, realizing frequency regulation of the grid terminal and improving the anti-disturbance performance of the power grid frequency.

## 2.2. Frequency Control Scheme of the Controllable Load

As shown in Figure 2, the controllable load frequency control scheme mainly consists of two sections. Firstly, the real-time load state is obtained and characteristic parameters of the load are calculated. The power router acquires and calculates the load group information at fixed time intervals. The time interval is represented by  $T$  ( $T = 1, 2 \dots, n$ ), there are  $n$  time intervals in a day, and the granularity of a time interval is 30 s. The load voltage amplitude and frequency of multiple output ports of the power router are monitored and collected during the time interval  $T$ . The load sensitivity of different ports is calculated using the collected parameters and the identification method. To fully and efficiently utilize the frequency regulation potential of the controllable load group, the frequency modulation capability of the load group needs to be evaluated. In this paper, the characteristic parameters of the multi-port load are calculated according to the load sensitivity. According to the characteristic parameters of variable voltage and variable frequency, the loads of different ports are controlled in a targeted manner.

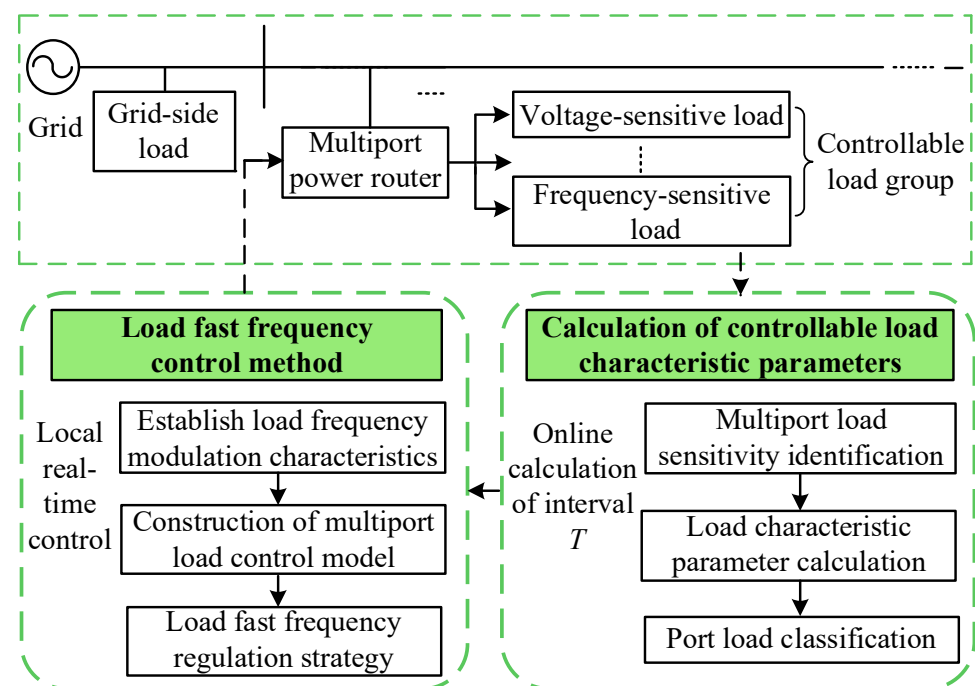


**Figure 2.** Frequency control scheme for the controllable load.

On the basis of the identified and calculated load characteristic parameters, a fast frequency control method is implemented. By embedding the proposed control algorithm into a local controller, real-time regulation of frequency can be achieved without centralized communication. Firstly, a frequency-regulation characteristic model of the total load that can respond to the frequency demand on the grid side is established. Then, the load power of the multi-port router is allocated in terms of the load characteristic parameters. In order to ensure that the load port responds to the grid frequency according to the power command of the frequency regulation characteristic, a multi-port load control model combined with the load characteristic parameters is established. By matching the control model and frequency modulation characteristics of the load port, the power router can

implement the load frequency modulation strategy according to the real-time operation state of the power grid and respond autonomously to grid changes in order to suppress frequency disturbances in the power grid.

### 3. Acquisition of the Controllable Load Characteristic Parameters

#### 3.1. Load Sensitivity Identification Method

Different controllable load groups have their inherent power consumption habits and power characteristics. In order to realize fast and unified control of load groups so that the load can compensate for the inertia support power missing from the grid, it is necessary to accurately obtain the real-time load characteristics such as load power and adjustable capacity.

The power function mathematical model describing the static load characteristics is

$$P = P_T \left( \frac{U}{U_T} \right)^{K_{pu}} \left( \frac{f}{f_T} \right)^{K_{pf}} \quad (1)$$

where  $P_T$  is the rated power of controllable load at  $T$ ;  $U_T$  and  $f_T$  are the rated voltage and frequency values to the port load at  $T$ , respectively.  $K_{pu}$  and  $K_{pf}$  are the load sensitivity of active power to voltage and active power to frequency, respectively.

Taking variable voltage load and variable frequency control as the research objects, and assuming that the system satisfies  $f = f_T$  at a steady-state time, the mathematical model of the variable voltage load characteristics can be obtained as follows:

$$P = P_T \left( \frac{U}{U_T} \right)^{K_{pu}} \quad (2)$$

When the controllable load voltage changes by  $\Delta U$ , the active power absorbed by the load will increase by  $\Delta P$ . At this time, the load model parameter identification formula can be obtained as

$$P = P_T + \Delta P = P_T \left( \frac{U_T + \Delta U}{U_T} \right)^{K_{pu}} = P_T \left( 1 + \frac{\Delta U}{U_T} \right)^{K_{pu}} \quad (3)$$

Formula (3) can be expanded according to the binomial theorem. Due to  $\Delta U < U_T$ , the formula expansion term of sensitivity index greater than or equal to 2 is far less than  $P_T$ . Therefore, the load characteristic model can be simplified to

$$P_U = P_{ln,T}^u \left( 1 + K_{pu} \frac{\Delta U}{U_T} \right) \quad (4)$$

where  $P_{ln,T}^u$  is the load-rated variable voltage power control in period  $T$ .

Similarly, when the frequency of controllable load changes by  $\Delta f$ , the mathematical model of load variable frequency characteristics can be written as

$$P_f = P_{ln,T}^f \left( 1 + K_{pf} \frac{\Delta f}{f_T} \right) \quad (5)$$

where  $P_{ln,T}^f$  is the load-rated variable frequency control power in the period  $T$ .

The load characteristics of AC ports and DC ports need to be identified. According to Formula (3), the sensitivity of the controllable load power to voltage and frequency at the AC port can be deduced separately as

$$\begin{cases} K_{pu} = \frac{\Delta P / P_{ln,T}^u}{\Delta U / U_T} \\ K_{pf} = \frac{\Delta P / P_{ln,T}^f}{\Delta f / f_T} \end{cases} \quad (6)$$

The controllable load of the DC port only considers static voltage characteristics, so its sensitivity model can be given by

$$\begin{cases} P_{Udc} = P_{dc,T}(1 + K_{pudc} \frac{\Delta U}{U_{dc,T}}) \\ K_{pudc} = \frac{\Delta P/P_{dc,T}}{\Delta U/U_{dc,T}} \end{cases} \quad (7)$$

where  $P_{dc,T}$  is the rated power of the DC port load in the period  $T$  and  $K_{pudc}$  is the sensitivity to frequency of the DC port load active power.

### 3.2. Calculation of Controllable Load Characteristic Parameters

Controllable loads have the characteristics of time variation and uncertainty. The identification method of load sensitivity can characterize the characteristics of group controllable loads. On this basis, in order to develop the frequency regulation ability of a controllable load adequately, it is necessary to obtain the adjustable degree of the port load. According to the above sensitivity identification results, it can be deduced that the controllable load adjustment depths of the AC and DC ports are, respectively:

$$\Delta P_{acmax} = K_{pu} P_{in,T}'' \frac{\Delta U_{max}}{U_T} + K_{pf} P_{in,T}^f \frac{\Delta f_{max}}{f_T} \quad (8)$$

$$\Delta P_{dcmax} = K_{dcpu} P_{dc,T} \frac{\Delta U_{dcmax}}{U_{dc,T}} \quad (9)$$

where  $\Delta U_{max}$  and  $\Delta f_{max}$  are the maximum adjustable range of voltage and the frequency of the controllable load under the AC port, respectively, and  $\Delta U_{dcmax}$  is the maximum voltage regulation range of the DC port load.

The participation of controllable loads in frequency regulation cannot affect the normal life and work needs of users. To ensure the reliability of user power quality at the load end and the stability of controllable load operation, the constraint boundary condition of the variable voltage characteristics is set as  $\Delta U_{max} = 7\% U_T$  in this paper. That is, the adjustable amount of the load voltage does not exceed 7% of the rated voltage. A constraint boundary condition is also set on the variable frequency, given as  $\Delta f_{lmax} = 0.5$  Hz. Similarly, the adjustment parameters of all load ports must satisfy these basic constraint conditions.

The output control of the power router needs to be based on the identification result of the load. To improve the availability of the load and the effect of frequency regulation according to the variable frequency and voltage characteristics of the load, the frequency or voltage control command matching the load end is selected to implement control. According to the adjustable depth of the AC and DC load, the power value of the output port can be further allocated reasonably.

## 4. Control Strategy of Frequency Modulation for Controllable Load

### 4.1. Frequency Modulation Characteristics of Controllable Load

When the controllable load is in a stable operation state, the output power of the load port is controlled by reasonably adjusting the load control parameters without affecting its normal operation. When the DC bus receives a power change from the output port on the controlled load side, the feedback power results in a change of bus voltage. In this case, the response of controllable load power to the grid end can be realized through the DC bus voltage stability control. Therefore, the content of this section mainly establishes the frequency regulation characteristics for the power router port and designs the load-side control according to power demand matching the frequency regulation characteristics so as to establish the connection between the grid and load side and realize the autonomous controllable load response to frequency changes in the grid. Before traditional primary frequency regulation action occurs, the controllable load responds quickly to give the grid inertial support, thereby realizing local frequency control without centralized communication.

As the grid disturbance or other factors will cause the grid frequency to fluctuate slightly, the controllable load frequency-control dead zone is set to consider these fluctuations. On the one hand, it avoids the problem of frequent charging and discharging of the DC bus caused by small fluctuations; on the other hand, it avoids the problem of an unstable load state caused by frequent control and power interference on the load side. The characteristic relationship between controllable load power and grid frequency is expressed as

$$\begin{aligned}
 P_{\text{Iset}} &= P_{\text{In},T} \\
 P_{\text{Iset}} &= P_{\text{In},T} + K_j(f_n - f_g) && \begin{aligned} &|f_g - f_n| < f_d \\ &f_d \leq |f_g - f_n| < f_{\text{mar}1} \\ &\text{or } f_{\text{mar}1} \leq |f_g - f_n| < f_{\text{mar}2} \end{aligned} \\
 P_{\text{Isetmax}} &= P_{\text{In},T} + \Delta P_{\text{Imax}} && f_g \geq f_{\text{mar}2} + f_n \\
 P_{\text{Isetmin}} &= P_{\text{In},T} - \Delta P_{\text{Imax}} && f_g \leq f_n - f_{\text{mar}2}
 \end{aligned} \tag{10}$$

where  $P_{\text{Iset}}$  is the total power command value of the load port;  $P_{\text{In},T}$  is the total rated state power of load in the period  $T$ ; and  $K_j(j = 1, 2)$  is the frequency modulation characteristic coefficient of the total load power frequency characteristic when the  $j$  strategy is adopted. The coefficient is calculated and taken according to the load identification result in the scenario of each period;  $f_n$  is the grid steady-state frequency;  $f_g$  is the actual frequency of the grid;  $f_{\text{mar}1}$  is the boundary frequency of the interval I;  $f_{\text{mar}2}$  is the boundary frequency of the interval II;  $f_d$  is the frequency modulation dead zone, which is set at 0.02 Hz; and  $\Delta P_{\text{Imax}}$  is the maximum adjustable amount of controllable load power,  $\Delta P_{\text{Imax}} = \Delta P_{\text{acmax}} + \Delta P_{\text{dcmax}}$ .

The equivalent schematic diagram of frequency modulation characteristics of the integrated load is shown in Figure 3. The controllable load does not involve modulation within the grid deadband frequency. The frequency modulation coefficient of the strategy in interval I is  $K_1$ . The frequency modulation coefficient of the interval II strategy is  $K_2$ . The established load characteristic model lays the foundation for the control of the port load in the following sections. The calculation of  $K_j$  is related to the control strategy, which will not be repeated here. The specific calculation method and tuning are described later.

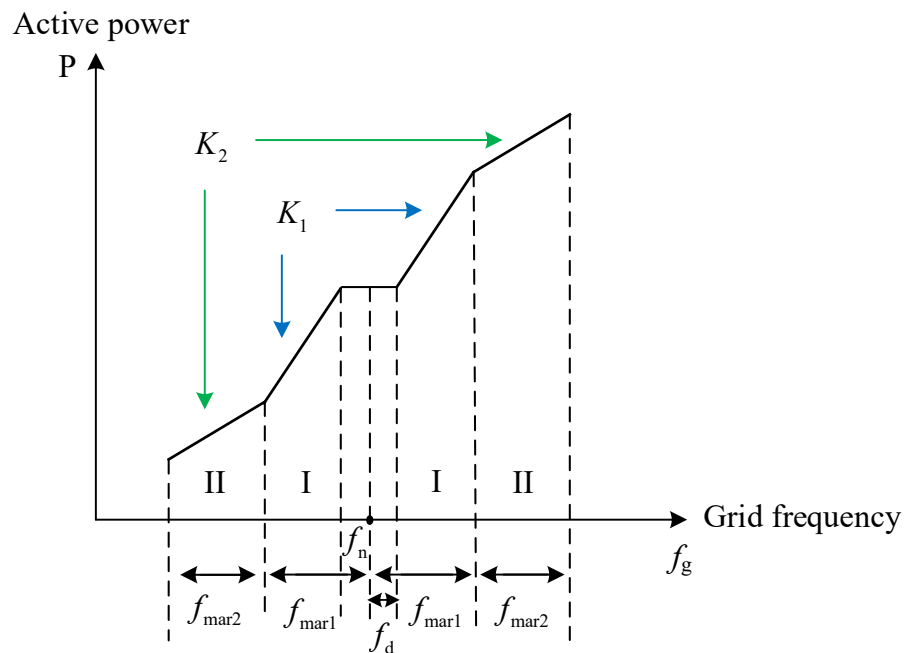


**Figure 3.** Schematic diagram of the integrated frequency modulation characteristic curve of the controllable load.



When the grid frequency fluctuates, the controllable load first participates in the frequency regulation response. Conventional generators also participate in primary frequency modulation.

The frequency modulation model for a grid-side generator that exhibits droop characteristics is given by

$$P_{Gset} = P_n + K_G (f_n - f_g) \tag{11}$$

where  $P_n$  is the rated power of the grid-side generator;  $P_{Gset}$  is the active power reference value of the generator; and  $K_G$  is the primary frequency modulation coefficient of the generator.

#### 4.2. Local Frequency Control Method for Multi-Port Controllable Load

Considering that the load group characteristics of each port are different, the control of the controllable load should not only respond to the frequency fluctuation of the power grid, but also ensure that the output power of the controlled multi-port load is within the adjustable range. Therefore, the control parameter  $K_j M_{i,j}$  of the established  $P - f$  characteristic and the load-side output control need to match the real-time load operating state. According to the result of load identification and the established controllable load characteristic formulas (10), the load frequency control models of the DC/AC port are proposed respectively, as shown in Figure 4.

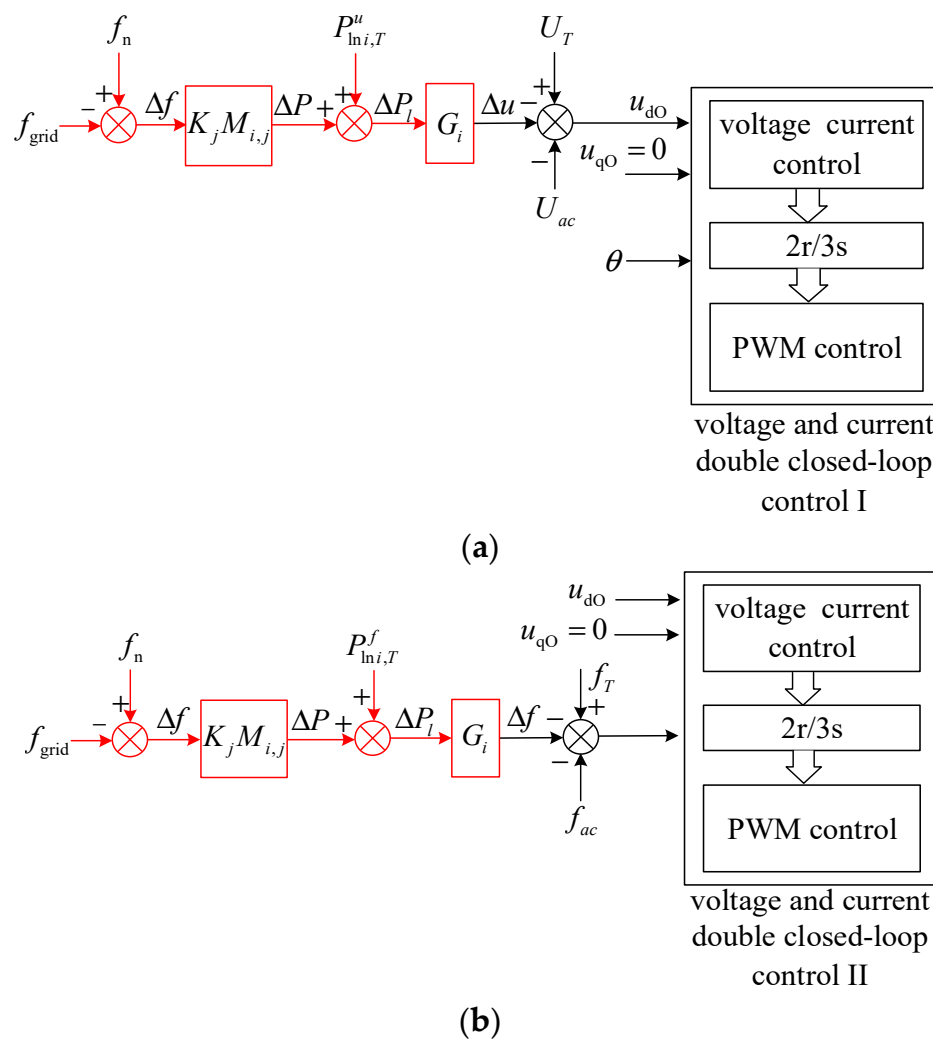


**Figure 4.** Schematic diagram of frequency modulation control for the controllable load: (a) variable voltage control, (b) variable frequency control.

Figure 4a shows the variable voltage control.  $f_{\text{grid}}$  is the actual frequency at the grid end;  $U_{ac}$  and  $f_{ac}$  are the measurement values of the voltage and frequency of the AC ports, respectively;  $U_T$  is the rated value of the port voltage; and  $\omega$  is the frequency reference value. For load variable voltage control, in order to ensure the stability of the port frequency  $f$ , the frequency of the dq transformation is controlled at 50 Hz, so  $\omega = 100\pi$ ; Figure 4b shows variable frequency control; voltage of the load port  $u_{dO}$  is controlled at 380 V.  $f_T$  is the rated value of the load port frequency.  $P_{lni,T}^u$  and  $P_{lni,T}^f$  are the rated power of the voltage- and frequency-sensitive load at port  $i$ . Where  $i = 1, 2, \dots, s$ , the router has  $s$  load ports in total.  $K_j M_{i,j}$  is the equivalent frequency modulation coefficient of the multi-port controllable load, where  $j$  indicates the adopted  $j$  strategy. The specific value of the frequency modulation coefficient  $K_j M_{i,j}$  is determined by the control strategy in the next section.

The load frequency control model obtains the power command value according to the power frequency characteristic of the load response to the grid side. Then, based on the identification results, the  $G$  link of the load-side control model is established. It can be concluded that  $G$  links of variable voltage and variable frequency control are  $\frac{U_T}{K_{pui} P_{lni,T}^u}$  and  $\frac{f_T}{K_{pfi} P_{lni,T}^f}$ , respectively. Finally, the load power change is controlled by adjusting the controllable variables of the DC-AC converter ports, thereby realizing local autonomous frequency modulation control of the load.

Similarly, the control of the DC port should meet both the power demand of the grid side and the load's adjustable capacity. The frequency modulation control diagram of the DC port is shown in Figure 5, where  $G_i = \frac{U_{dc,T}}{K_{dcpui,T} P_{dci,T}^u}$ .  $U_{dc}$  is the voltage measurement value;  $U_{dc,T}$  is the rated value of the port voltage.

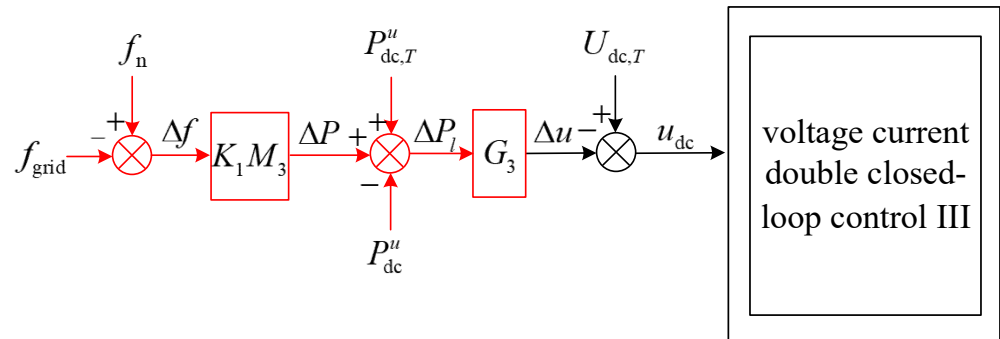


Figure 5. Schematic diagram of frequency modulation control of the DC port controllable load.

### 4.3. Frequency Modulation Control Strategy of Multi-Port Controllable Load

When the power grid is disturbed, the controllable load can adjust its own operating state by controlling its port voltage or frequency value. Considering the need for orderly control of multi-port loads and reasonable power distribution, the proposed strategy first prioritizes AC load variable voltage control. On one hand, because the response of the frequency-sensitive load has inertia, its response rate is slower than that of the voltage-sensitive load when grid disturbance occurs. On the other hand, the recovery time after the frequency-sensitive load participates in the grid frequency regulation is longer. Moreover, the response of the controllable load to small disturbances of the power grid needs to leave a certain margin. Otherwise, when the remaining capacity is insufficient, the problem of lack of frequency regulation will occur in the face of special situations such as large disturbances. Accordingly, the controllable load frequency modulation control strategy is divided into two stages. This strategy preferentially regulates the voltage-sensitive load, therefore setting the variable voltage instruction equal to  $0.5 \Delta U_{\text{max}}$  as the judgment condition for strategy switching. When this threshold is exceeded, other loads are regulated to participate in the response.

Control of the controllable load should be based on load-characteristic parameters. Therefore, after the control strategy is started, it detects whether the power grid is initially operating in a stable state. If the power grid is stable, the load identification is performed first. The identification can be carried out at most once in a period  $T$ . Then, when the detected grid frequency is disturbed and changes to the response range  $f_{\text{mar}1}$  are noted, at this time, if identification is under way, the identification control shall be terminated immediately, the frequency modulation control shall be preferentially entered, and frequency regulation strategy 1 is started.

Strategy 1 sets only the load's variable voltage control to participate in the response. The adjustable voltage range of the load is  $0.5 \Delta U_{\text{max}}$ . According to the identification results, the maximum frequency modulation interval  $\Delta f_{\text{max}}$  and the adjustable depth of the load's variable voltage are taken as boundary conditions, where, letting  $\Delta f_{\text{max}} = (f_{\text{mar}1} + f_{\text{mar}2}) = 0.2$  Hz, the number of voltage-sensitive load groups is  $m$ . The variable frequency modulation coefficient  $K_1$  can be obtained as shown in Equation (12).

$$K_1 = \frac{\sum_{i=1}^m K_{\text{pui}} P_{\text{ln}i,T}^u \Delta U_{\text{max}}}{\Delta f_{\text{max}} U_T} \quad (12)$$

The realization of frequency regulation control needs to reasonably distribute the power to the different load ports of the power router. In order to ensure that the load output degree under different power router interfaces is as balanced as possible, the load power of the variable voltage and frequency ports are allocated according to the proportion of the adjustable depth of each port. Corresponding load characteristic models are established for different ports; let  $P_{i,j}^*$  ( $i = 1, 2, \dots, s; j = 1, 2$ ) represent the load power of  $i$  port  $j$  strategy. According to the sensitivity identification and the total power frequency characteristic formula, the load variable voltage characteristic model of strategy 1 can be obtained:

$$P_{i,1}^* = P_{\text{ln}i,T}^u + K_j (f_g - f_n) M_{i,1} \quad (13)$$

where ( $i = 1, 2, \dots, m; j = 1$ ),  $M_{i,j}$  represents the ratio of the capacity of the controllable load that can participate in frequency regulation to the total capacity at the  $j$ -th strategy of the  $i$ -th port, and represents the frequency regulation capability of the port. Therefore, for the variable voltage control of strategy 1, there are

$$M_{i,1} = K_{\text{pui}} P_{\text{ln}i,T}^u \frac{\Delta U_{\text{max}}}{U_T} / \Delta P_{l_{m,1}} \quad (14)$$

where  $\Delta P_{l_{m,j}}$  is the adjustable depth for total load for the selected participating in frequency modulation ports when the  $j$  th strategy is adopted; when using only voltage regulation control, the variable voltage load can be obtained:  $\Delta P_{l_{m,1}} = \left( \sum_{i=1}^m K_{\text{pui}} P_{\text{ln}i,T}^u \Delta U_{\text{max}} \right) / U_T$ .

According to the established load power frequency characteristics, the frequency modulation coefficient  $K_1$  of the port calculated above and other voltage transformation control parameters  $M_{i,j}$  and  $G_i$  are assigned to the corresponding AC port to realize local real-time fast frequency modulation.

Based on the above strategy, the controllable voltage is taken as the judgment condition. If the grid frequency is disturbed and the voltage regulation keeps increasing until it reaches  $0.5 \Delta U_{\text{max}}$ , control strategy 2 will start. In the frequency II interval, the port of the converter is controlled by variable voltage and variable frequency. In order to suppress frequency disturbance as much as possible in this interval, the strategy is to control all loads in order to fully participate in frequency regulation. By doing so, the effect of the load power smoothly and fully participating in the frequency modulation over the whole frequency range is realized. The frequency modulation coefficient of this interval is  $K_2$ , which is determined by the adjustable depth of the total controllable load in interval II and the maximum adjustable

range of the grid frequency as boundary conditions. Let  $f_{mar2} = 0.1$  Hz.  $K_2$  can be obtained as shown in Equation (15).

$$K_2 = \sum_{i=1}^m K_{pui} P_{ln i,T}^u \frac{\Delta U_{max}}{2U_T f_{mar2}} + \sum_{i=m+1}^{m+q} K_{pfi} P_{ln i,T}^f \frac{\Delta f_{max}}{f_T f_{mar2}} + \sum_{i=m+q+1}^{m+q+r} K_{dcpui} P_{dci,T}^u \frac{\Delta U_{max}}{U_T f_{mar2}} \tag{15}$$

where  $m$  is the number of ports for voltage-sensitive loads,  $q$  is the number of ports for frequency-sensitive loads, and  $r$  is the number of ports for DC loads.

Similarly, when strategy 2 is adopted ( $j = 2$ ), the multi-port AC–DC load power frequency characteristic model is given as

$$\begin{cases} P_{i,j}^* = P_{ln i,T}^u + 0.5K_1 M_{i,1} (\pm \Delta f_{max}) + K_2 (f_g - f_n \pm f_{mar1}) M_{i,2} \\ \quad (i = 1, \dots, m; j = 2) \\ P_{i,j}^* = P_{ln i,T}^f + K_2 (f_g - f_n \pm f_{mar1}) M_{i,2} \\ \quad (i = m + 1, \dots, m + q; j = 2) \\ P_{i,j}^* = P_{dci,T}^u + K_2 (f_g - f_n \pm f_{mar1}) M_{i,2} \\ \quad (i = m + q + 1, \dots, m + q + r; j = 2) \end{cases} \tag{16}$$

When  $f_g > f_n$ , the “±” in the formula is the “–” sign; when  $f_g < f_n$ , the “±” in the formula is the “+” sign; where

$$\begin{cases} M_{i,j} = 0.5K_{pui} P_{ln i,T}^u \frac{\Delta U_{max}}{U_T \Delta P_{ls,j}} & (i = 1, \dots, m) \\ M_{i,j} = K_{pfi} P_{ln i,T}^f \frac{\Delta f_{max}}{f_T \Delta P_{ls,j}} & (i = m + 1, \dots, m + q) \\ M_{i,j} = K_{dcpui} P_{dci,T}^u \frac{\Delta U_{max}}{U_T \Delta P_{ls,j}} & (i = m + q + 1, \dots, m + q + r) \end{cases} \tag{17}$$

In strategy 2, the whole load participates in frequency regulation, and the total load adjustment depth  $\Delta P_{ls,2}$  is  $\Delta P_{ls,2} = (0.5 \sum_{i=1}^m K_{pui} P_{ln i,T}^u \Delta U_{max}) / U_T + (\sum_{i=m+1}^{m+q} K_{pfi} P_{ln i,T}^f \Delta f_{max}) / f_T + (\sum_{i=m+q+1}^{m+q+r} K_{dcpui} P_{dci,T}^u \Delta U_{max}) / U_T$ .

Local real-time frequency modulation control is realized by assigning the calculated variable voltage and frequency control parameters  $M_{i,2}$  and  $G_i$  of the port and the frequency modulation coefficient  $K_2$  to the corresponding AC and DC ports.

In summary, based on load characteristic identification and combined with the proposed control method, a local real-time frequency modulation control strategy is realized. In Figure 6, a schematic diagram of the frequency modulation strategies within the cycle  $T$  is given.

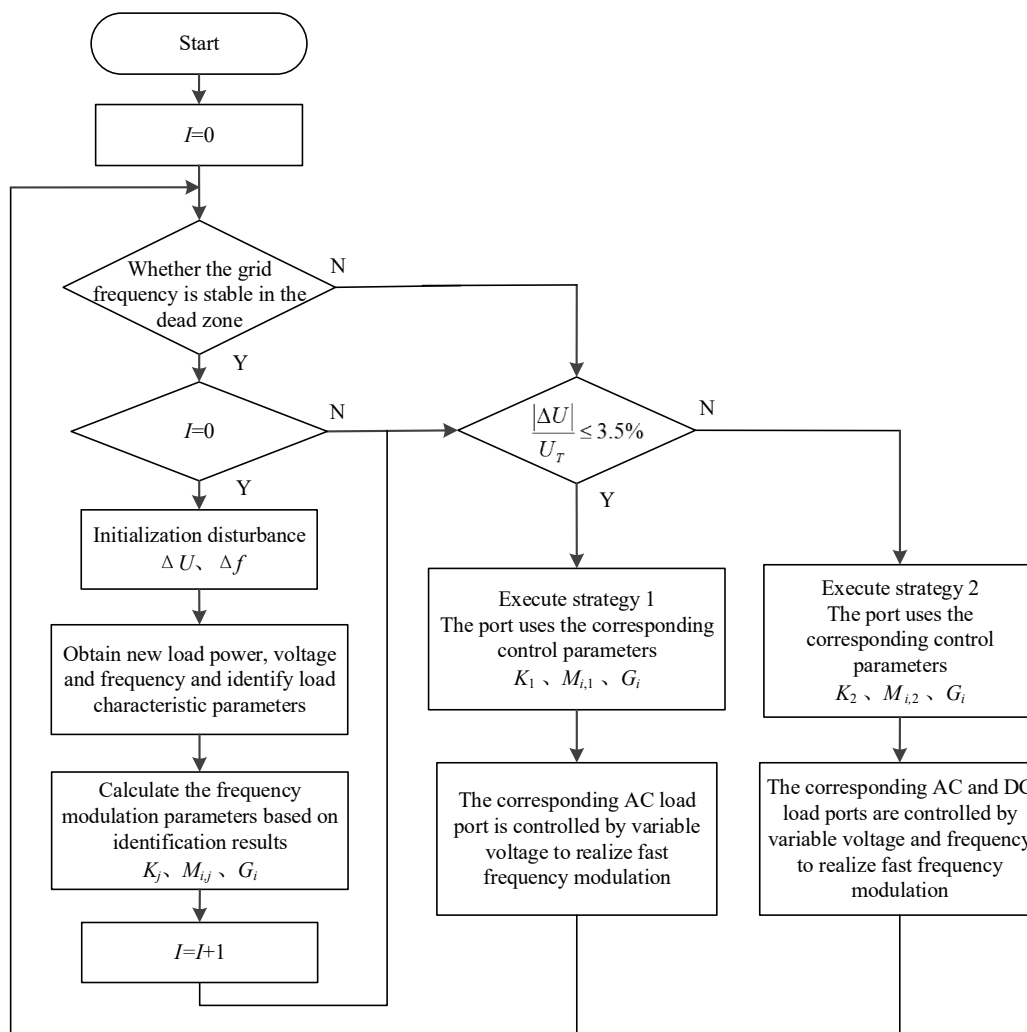


**Figure 6.** Flow chart of frequency control strategies for a multi-port controllable load.

## 5. Simulation Validation and Analysis

In order to verify the feasibility and effectiveness of the proposed method, Matlab/Simulink software was used for simulation research. Controllable loads were connected to the grid through the multi-port power router. The simulation system's topology structure is shown in Figure 1. The power router was equipped with three load ports. The two AC output ports are connected to voltage- and frequency-sensitive load groups, and the DC ports access the load group sensitive to voltage. DC stabilization control was used on the power router rectifier side to ensure stability of the bus voltage. The output end of the power router selected the control method for the load characteristics of the matching port according to the load frequency adjustment strategy, so that the frequency response to it when the power grid was disturbed was rapid.

In the simulation, an AC/DC rectifier was set at the grid-connected end of the power router, and two DC/AC inverters were set at the load side, using the three-phase bridge inverter structure. The DC port used a DC/DC converter. The DC/DC output voltage rating was 380 V. The router's common DC bus capacitance was  $C_{bus} = 750 \times 10^{-6}$  F. The valid value range of the three-phase line voltage of the power router input port was  $380 \pm 26$  V and the frequency range was  $50 \pm 0.5$  Hz; the DC bus voltage rated value was 850 V; the range of the three-phase AC line voltage effective value and DC port output voltage was  $380 \pm 26$  V; and the AC controllable frequency range was  $50 \pm 0.5$  Hz. On the grid side, the filter inductance was  $L_1 = 1.1 \times 10^{-3}$  H and the capacitor was  $C_1 = 30 \times 10^{-6}$  F. The filter inductance and capacitance of the AC output port of the power router were

$L_2 = L_3 = 1.6 \times 10^{-3}$  F and  $C_2 = C_3 = 22 \times 10^{-6}$  H, respectively. The filter parameters of the DC port were  $L_4 = 1.3 \times 10^{-3}$  F and  $C_4 = 35 \times 10^{-6}$  H. The generator used a three-phase simplified synchronous machine; its rated capacity was  $12 \times 10^4$  W, rated line voltage 380 V, and rated frequency 50 Hz. Generator power was 47 kW and the generator droop parameters were  $k_{sg} = 1.8 \times 10^4$  and  $J = 0.67$  kg/m<sup>2</sup>. The response delay of the generator's primary frequency modulation was set to 0.25 s. Grid-connected PV power generation was 10 kW. Two load scenarios were set to compare the frequency modulation effect. The load parameters in Scenario 1 were as follows: 37 kW for the grid-side load and 20 kW for the controllable AC voltage-sensitive load. Scenario 2 load parameters were as follows: the grid-side load was 30 kW, the controllable AC voltage-sensitive load was 10 kW, the frequency-sensitive load was 12 kW, and the DC variable voltage load was 5 kW.

The frequency modulation control strategy needed to obtain the real-time running state and characteristic parameters of the load. The strategy started at 3 s. After the system was detected to be stable, the load frequency and voltage characteristic coefficient were identified. The port load voltage and frequency changes were controlled, and small perturbations of 0.1 Hz and  $0.02 U_T$  were applied to the port. The identification results obtained after stabilization are shown in Table 1. According to the comparison of simulation identification value and theoretical value, it can be seen that the identification result is basically accurate. The average error is about 2.13%.

**Table 1.** Identification results of characteristic parameters of load.

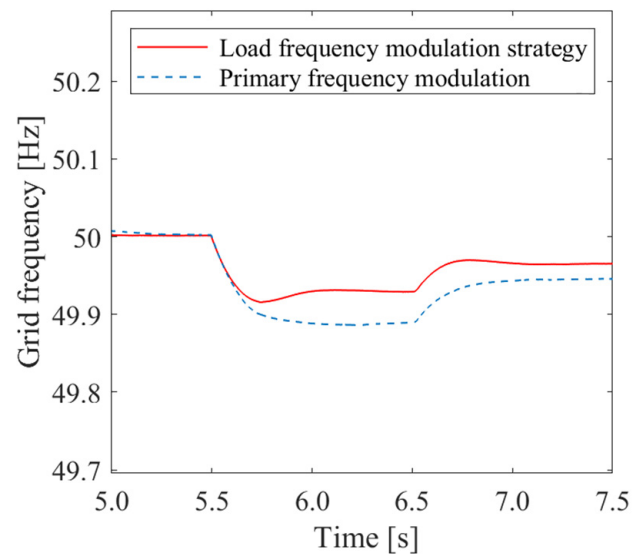
Sensitivity	Voltage-Sensitive Loads $K_{pu}$	Frequency-Sensitive Loads $K_{pf}$	DC Loads $K_{pudc}$
Identification value	1.52	2.41	1.97
Theoretical value	1.50	2.50	2.00
Identification error	1.3%	3.6%	1.5%

### 5.1. Validation of Variable Voltage Load Participating in Frequency Modulation Strategy

The simulation was carried out when the grid frequency was disturbed. The simulation conditions were as follows: The load group of Scenario 1 was adopted. The initial operation of the grid was in a stable state, and the grid side load was set to increase by 2 kW at 5.5 s. At 6.5 s, the load suddenly decreased by 1 kw. According to the identification results, the frequency modulation coefficient of the variable voltage control was calculated as 20,000. Because the grid-side disturbance was small and the strategy-switching condition was not reached, the strategy 1 load variable-voltage control was adopted according to the judgment of the power router.

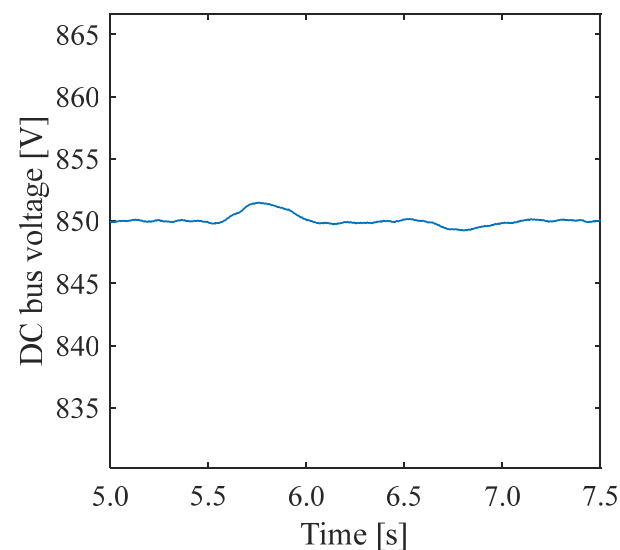
The grid frequency results are shown in Figure 7, compared with the control strategy and traditional primary frequency modulation. At 5.5 s, the power grid frequency drops due to the load surge. Comparing the two frequency modulation control curves, it can be seen that the controllable load can quickly provide frequency support for the power grid at the initial stage of the disturbance, so as to quickly suppress the frequency mutation. At 5.75 s, the frequency of strategy 1 was basically suppressed and recovered slightly. This is because at this time, in addition to the controllable load, primary frequency modulation control also starts to participate in the response. Under the proposed control strategy, the frequency after disturbance is restored to 49.93 Hz, while under the traditional frequency modulation method, the frequency is restored to 49.89 Hz. At 6.5 s, the disturbance load decreases by 1 kW and the grid frequency starts to rise. Finally, the frequency is restored to 49.97 Hz under the proposed strategy, and the final value of the frequency under the traditional frequency modulation control is 49.95 Hz. It can be seen that at 5.75 s, the strategy basically suppresses the decreasing trend of the frequency, which is faster than the stable speed of traditional frequency modulation. Evidently, the fast frequency modulation control method can not only suppress the frequency mutation rate of the load but also

reduce the amplitude of frequency change and provide a superior response time for primary frequency modulation and other control methods.



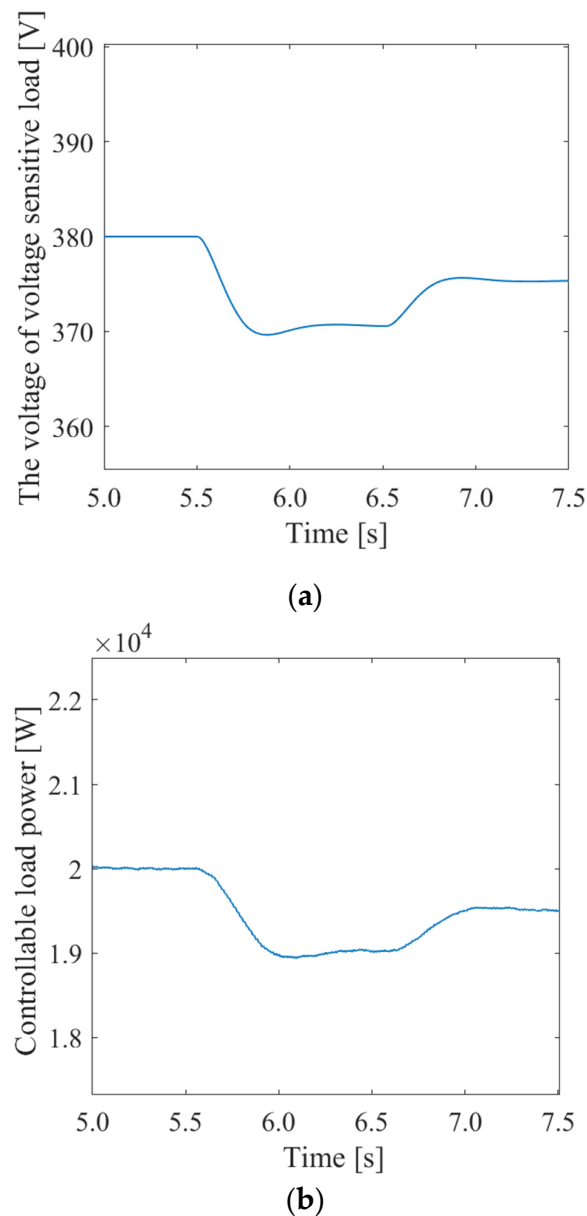
**Figure 7.** Comparison of grid frequency between the proposed strategy and traditional control.

Figure 8 shows the DC bus voltage of the proposed control strategy. The bus voltage fluctuates slightly at the time of disturbance and quickly recovers to 850 V with good overall stability.



**Figure 8.** DC bus voltage under the proposed control strategy.

Figure 9a,b show the voltage value and power of the port load, respectively. At 5.5 s, the grid frequency increases, the controllable load responds quickly, and the port voltage drops to 370.6 V. The port output power is 19.03 kW. At 6.5 s, the port voltage rises to 375.3 V and the port output power is 19.52 kW. The proposed control strategy can effectively alleviate the impact of load disturbance on the grid frequency, and the effect is better than that of the traditional frequency modulation method.



**Figure 9.** Variable voltage control results: (a) load voltage, (b) load power.

### 5.2. Validation of Multiport Load Participating in Frequency Modulation Strategy

To verify the effectiveness of the proposed strategy, a relatively large disturbance scenario was set for simulation where the load group of Scenario 2 was adopted. The initial operation of the grid was in a stable state. The disturbance occurred at 5.5 s, the grid side load dropped by 3 kW, and the photovoltaic power increased 1 kW. The disturbance power recovered at 6.5 s. According to the identification results, the calculated frequency modulation coefficient of the variable voltage control was 15,000, the frequency modulation coefficient of the variable frequency control was 3000, and the frequency modulation coefficient of the DC port was 10,000. At the beginning of the disturbance, strategy one was adopted. When the voltage reached 3.5%  $U_T$ , the grid-side disturbance was judged to be large according to the power router, and strategy two was adopted, in which all the controllable loads participate in the frequency modulation control.

The result of the frequency modulation is shown in Figure 10. At 5.5 s, the disturbance makes the grid frequency rise. Under the load frequency modulation strategy, the frequency is basically restored to stability at 5.75 s, and the stable frequency is 50.146 Hz. However, the traditional FM control gradually stabilized at 6.1 s, and the stable frequency was



50.22 Hz. Under the traditional control, the frequency has exceeded the allowable frequency extremum, which greatly increases the risk of system instability. It can be seen that the proposed strategy can quickly suppress frequency mutation and the frequency fluctuation is smaller.

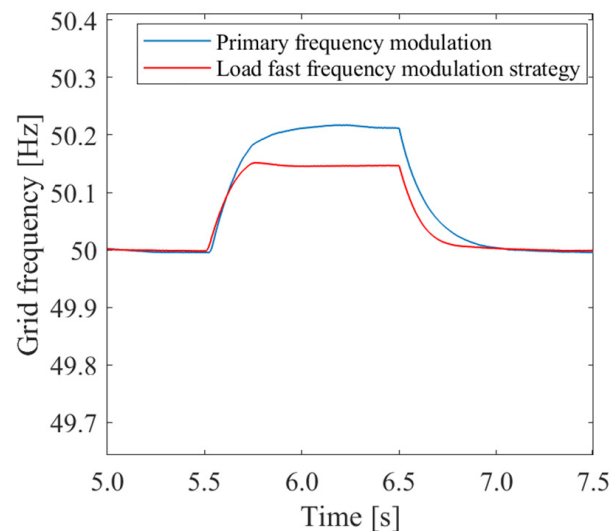


**Figure 10.** Comparison of grid frequency between the control strategy and the traditional method.

Figure 11 shows the DC bus voltage under the proposed control strategy. The bus voltage fluctuates about 2.5 V at the time of disturbance and quickly recovers to 850 V, with good overall stability. Figure 12a,b show the voltage and frequency control results of the AC port, respectively. Figure 12c shows the DC port voltage. As can be seen in Figure 12, only AC voltage regulation control is started at 5.5 s. At around 5.62 s, control strategy 2 starts, and then the voltage and frequency parameters of Figure 12b,c begin to increase from the rated value. It can be seen that the voltage amplitude is stable at about 5.8 s. The frequency is stable at 6 s. This is due to the inertial response characteristics of the variable frequency load itself; the frequency changes more slowly than the voltage amplitude. The stable values of the control parameters of the three ports are 398.7 V, 50.23 Hz, and 394.2 V.

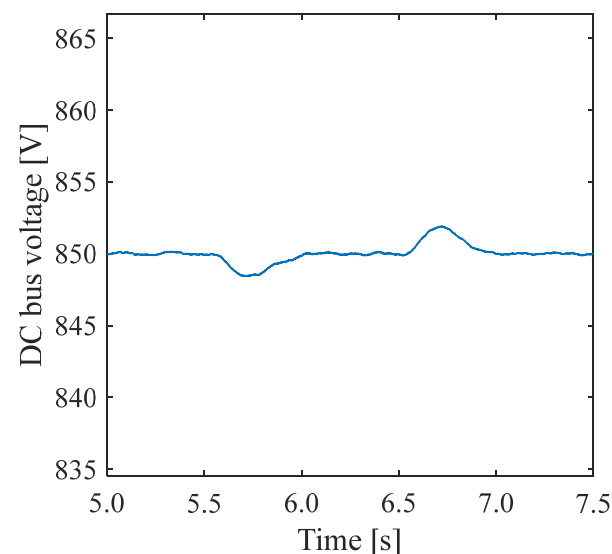
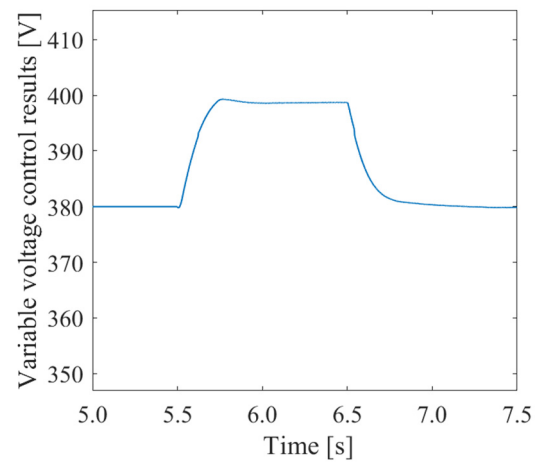
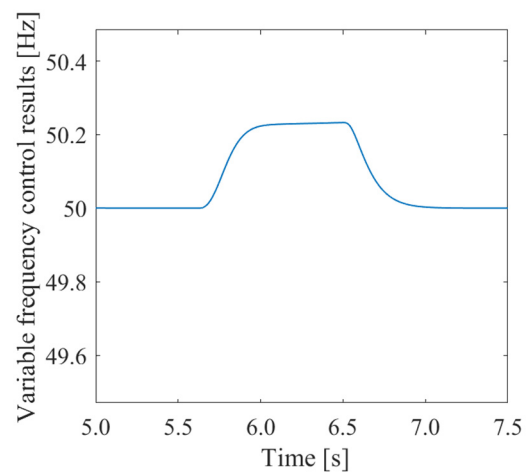


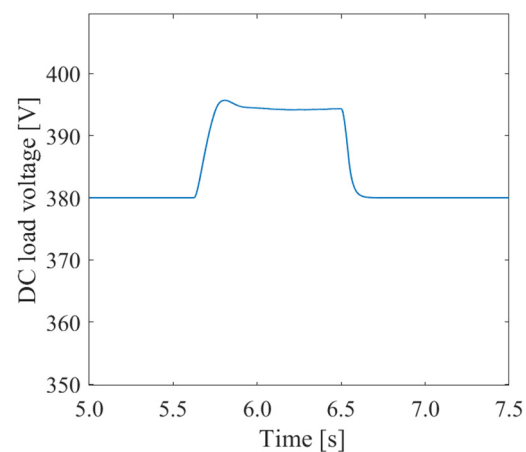
**Figure 11.** DC bus voltage.



(a)



(b)

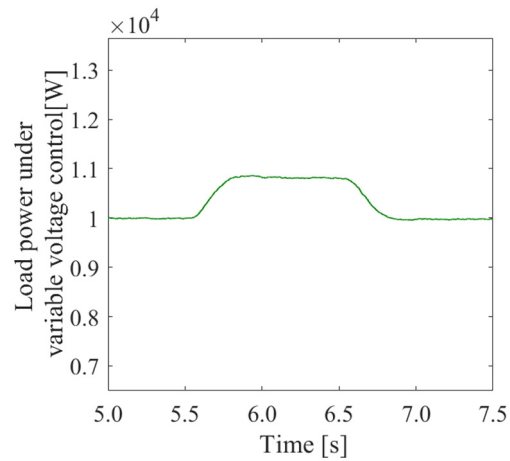


(c)

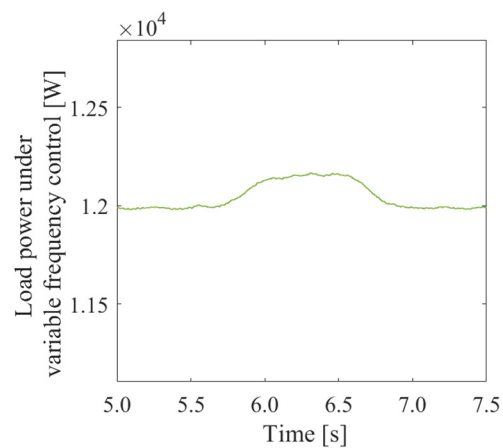
**Figure 12.** Multi-port load control parameters: (a) variable voltage control, (b) variable frequency control, (c) DC voltage control.

Figure 13a,b show the load power variation of the AC port variable voltage and variable frequency controls, respectively. Figure 13c shows the DC port power value.

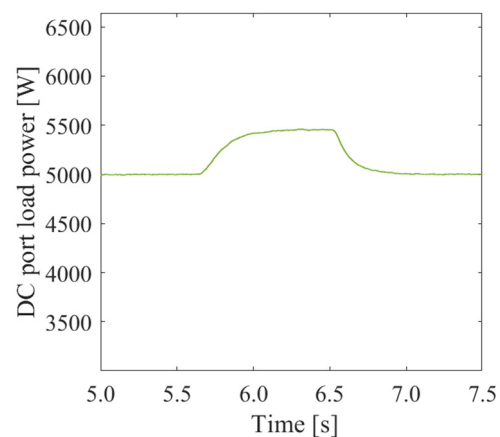
Figure 13a shows port power changes from 5.5 s. In Figure 13b,c, the power value of the port starts to respond at around 5.62 s. According to the control, the load power change of frequency conversion control is obviously slower than that of other ports. The stable values of the three ports are 10.08 kW, 12.15 kW, and 0.545 kW, respectively.



(a)



(b)



(c)

**Figure 13.** Multi-port load power: (a) variable voltage control, (b) variable frequency control, (c) DC voltage control.

After the disturbance was generated, the power consumed by the load of the three ports increased, which restrained the impact of the disturbance. The simulation results

show that, compared with the traditional frequency modulation method, the frequency fluctuation of the power grid is obviously suppressed when the proposed controllable load frequency modulation strategy is adopted. The controllable load can provide fast support for the grid frequency so as to promote the stability of the power grid.

## 6. Conclusions

This research proposes a local frequency modulation control strategy of controllable load characteristic identification in a multi-port power router and draws the following main conclusions:

1. The static identification model of the controllable load is established and applied to the frequency modulation problem in a multi-port router. The load identification is carried out by applying small signals to different port loads. The identification method can effectively calculate the load sensitivity and load characteristic parameters of variable voltage and frequency. It lays the foundation for the load's fast local frequency modulation control;
2. A multi-port controllable load control method based on a power router is established in this paper. This method can be applied to both AC and DC ports of power routers, and the corresponding variable voltage and variable frequency control can be given for different port loads. This method can realize the purpose of fast local frequency modulation without communication. The topology structure adopted here can realize the transmission of load power through voltage control of the DC bus and maintain the stable work of the power router. The power frequency characteristics established for the model match the grid-side and load-side power demands. By controlling the voltage amplitude and frequency of a load port, the load can autonomously respond to power grid frequency;
3. A multi-port, controlled-load frequency control strategy is proposed, and the frequency modulation coefficient which can adapt to the load state is designed. The adjustment margin of the load in the adjustable frequency segment is ensured. According to the characteristic parameters of varying load between periods, the frequency modulation capacity of different ports can be reasonably allocated. This strategy can enable the controllable load to participate in the frequency modulation response fully and smoothly in the adjustable frequency segment. At different stages, each load port can respond reasonably according to the frequency modulation coefficient. This strategy can make the load perform its frequency modulation response quickly in the early stage when the frequency of the grid is disturbed, fill the inertial vacant power of the grid, and provide support for the frequency of the grid. It can also buy time for other power grid frequency modulation methods, such as primary frequency modulation. Finally, the effectiveness of the frequency modulation strategy is verified by simulation.

**Author Contributions:** C.L., data collection, preparation, creation, and presentation for thesis work and journal works, especially writing the initial draft, including translation; Q.J. and L.L., model design and simulation, application of statistical, mathematical, computational methods; J.C., paper revision, critical review, commentary, and revision. All authors have read and agreed to the published version of the manuscript.

**Funding:** This research was funded in part by National Natural Science Foundation of China, No. 51877186.

**Data Availability Statement:** Not applicable.

**Conflicts of Interest:** The authors declare no conflict of interest.

## Nomenclature

$L_1, L_2, L_3, L_4$	filter inductances of power router
$C_{bus}$	DC bus capacitance of power router
$U_{dc}$	command value of the DC bus voltage
$C_2, C_3, C_4$	filter inductances and capacitances
$R_{lu}, R_{lf}, R_{ldc}$	voltage- and frequency-sensitive load, DC load
$T$	power router control cycle
$P_T, U_T, f_T$	load rated power, voltage, and frequency at period $T$
$K_{pu}, K_{pf}$	voltage and frequency sensitivity of AC load
$P_{ln,T}^u, P_{ln,T}^f, P_{dc,T}$	power of variable voltage, variable frequency control load, and DC load
$K_{pudc}$	DC voltage sensitivity
$\Delta U_{max}, \Delta f_{max}, \Delta U_{dcmax}$	maximum adjustable range of voltage and frequency of AC controllable load, DC load maximum voltage adjustable range
$P_{lset}, P_{ln,T}$	total load power command value, total load rated power
$K_j$	total frequency modulation characteristic coefficient at $j$ strategy ( $j = 1, 2$ )
$f_n, f_g$	grid steady-state and actual frequency
$f_{mar1}, f_{mar2}$	interval I and interval II boundary frequencies
$f_d$	frequency modulation dead zone
$\Delta P_{lmax}$	maximum adjustable capacity of controllable load power
$P_n, P_{Gset}$	generator rated power and active power
$K_G$	frequency modulation coefficient of the generator
$U_{ac}, f_{ac}$	measurement values of voltage and frequency of AC ports
$P_{lni,T}^u, P_{lni,T}^f$	rated power of voltage- and frequency-sensitive load of AC port $i$
$K_{pui}, K_{pfi}, K_{dcpui,T}$	voltage and frequency sensitivity of load of AC port $i$
$P_{dci,T}^u$	rated power of voltage-sensitive load of DC port $i$
$U_{dc,T}$	rated voltage of DC port load
$\Delta f_{max}$	maximum frequency modulation interval
$P_{i,j}^*$	load power of $i$ port, $j$ strategy
$M_{i,j}$	frequency-regulation capability coefficient at $j$ strategy of $i$ port
$\Delta P_{lm,j}$	adjustable depth for total frequency modulation load at $j$ strategy

## References

1. Qi, Y.; Deng, H.; Wang, J.; Tang, Y. Passivity-Based Synchronization Stability Analysis for Power-Electronic-Interfaced Distributed Generations. *IEEE Trans. Sustain. Energy* **2020**, *12*, 1141–1150. [\[CrossRef\]](#)
2. Bulatov, Y.N.; Kryukov, A.V.; Arsentiev, G.O. Use of Power Routers and Renewable Energy Resources in Smart Power Supply Systems. In Proceedings of the 2018 International Ural Conference on Green Energy (UralCon), Chelyabinsk, Russia, 4–6 October 2018; pp. 143–148.
3. Margaritis, I.D.; Papathanassiou, S.A.; Hatziargyriou, N.D.; Hansen, A.D.; Sorensen, P. Frequency Control in Autonomous Power Systems with High Wind Power Penetration. *IEEE Trans. Sustain. Energy* **2012**, *3*, 189–199. [\[CrossRef\]](#)
4. Hua, X.; Hong, Y.X.; Na, L. Control strategy of DFIG wind turbine in primary frequency regulation. In Proceedings of the 2018 13th IEEE Conference on Industrial Electronics and Applications (ICIEA), Wuhan, China, 31 May–2 June 2018; pp. 1751–1755.
5. Sun, M.; Jia, Q.; Pei, Z.; Dong, C.; Wang, Z.H.; Jin, X. Advanced Frequency Support Strategy of Double-Stage Grid-Connected PV Generation. *J. Electr. Eng. Technol.* **2019**, *14*, 2239–2250. [\[CrossRef\]](#)
6. Chen, W.; Sun, N.; Ma, Z.; Liu, W.; Dong, H.; Su, M.A. A Two-Layer Optimization Strategy for Battery Energy Storage Systems to Achieve Primary Frequency Regulation of Power Grid. *Energies* **2018**, *16*, 2811. [\[CrossRef\]](#)
7. Wang, X.; Lin, C.; Shen, C.; Gan, W.; Wang, L. Control Strategy for Fast Frequency Modulation of Regional Power Grid with Energy Storage System. In Proceedings of the 2020 15th IEEE Conference on Industrial Electronics and Applications (ICIEA), Kristiansand, Norway, 9–13 November 2020; pp. 1226–1230.
8. Gheisarnejad, M.; Mohammadi-Moghadam, M.H.; Boudjadar, J.; Khooban, M.H. Active Power Sharing and Frequency Recovery Control in an Islanded Microgrid with Nonlinear Load and Nondispatchable DG. *IEEE Syst. J.* **2019**, *14*, 1058–1068. [\[CrossRef\]](#)
9. Yang, X.; Su, J.; Ding, M.; Du, Y. Research on Frequency Control for Micro-grid in Islanded Operation. *Power Syst. Technol.* **2012**, *34*, 164–168.
10. Gulzar, M.M.; Iqbal, M.; Shahzad, S.; Muqet, H.A.; Shahzad, M.; Hussain, M.M. Load Frequency Control (LFC) Strategies in Renewable Energy-Based Hybrid Power Systems: A Review. *Energies* **2022**, *15*, 3488. [\[CrossRef\]](#)
11. Jia, Y.; Dong, Z.Y.; Sun, C.; Meng, K. Cooperation-Based Distributed Economic MPC for Economic Load Dispatch and Load Frequency Control of Interconnected Power Systems. *IEEE Trans. Power Syst.* **2019**, *34*, 3964–3966. [\[CrossRef\]](#)

12. Ju, Y.; Du, Y.; Liu, H. Research Review of Flexible Load Aggregation Methods in Distribution Networks. In Proceedings of the 2020 IEEE 4th Conference on Energy Internet and Energy System Integration (EI2), Wuhan, China, 30 October–1 November 2020; pp. 3388–3393.
13. Yang, W.; Lin, C.; Ning, Q.; Liu, Y.; Wang, X. Review on Distribution Network Planning Methods Considering Large-scale Access of Flexible Load. In Proceedings of the 2018 2nd IEEE Conference on Energy Internet and Energy System Integration (EI2), Beijing, China, 20–22 October 2018; pp. 1–6.
14. Gholamrezaie, V.; Dozein, M.G.; Monsef, H.; Wu, B. An Optimal Frequency Control Method Through a Dynamic Load Frequency Control (LFC) Model Incorporating Wind Farm. *IEEE Syst. J.* **2018**, *12*, 392–401. [[CrossRef](#)]
15. Sun, Y.; Mao, Y.; Li, Z.; Zhang, X.; Li, F. A Comprehensive Clustering Method of User Load Characteristics and Adjustable Potential based on Power Big Data. *Proc. CSEE* **2021**, *41*, 6259–6271.
16. Carne, G.D.; Buticchi, G.; Liserre, M.; Vournas, C. Load Control Using Sensitivity Identification by Means of Smart Transformer. *IEEE Trans. Smart Grid* **2016**, *9*, 2606–2615. [[CrossRef](#)]
17. Carne, G.D.; Liserre, M.; Vournas, C. On-Line Load Sensitivity Identification in LV Distribution Grids. *IEEE Trans. Power Syst.* **2017**, *32*, 1570–1571. [[CrossRef](#)]
18. Reddy, C.P.; Chakrabarti, S.; Srivastava, S.C. A Sensitivity-Based Method for Under-Frequency Load-Shedding. *IEEE Trans. Power Syst.* **2015**, *29*, 984–985. [[CrossRef](#)]
19. Li, C.; Wu, Y.; Sun, Y.; Zhang, H.; Terzija, V. Continuous Under-Frequency Load Shedding Scheme for Power System Adaptive Frequency Control. *IEEE Trans. Power Syst.* **2019**, *35*, 950–961. [[CrossRef](#)]
20. Wu, X.; Xue, F.; Dai, J.; Tang, Y. Adaptive Under-Frequency Load Shedding Control Strategy of Power Systems with Wind Turbines and UHVDC Participating in Frequency Regulation. *Front. Energy Res.* **2022**, *10*, 541. [[CrossRef](#)]
21. Gu, W.; Liu, W.; Zhu, J.; Zhao, B.; Wu, Z.; Luo, Z. Adaptive Decentralized Under-Frequency Load Shedding for Islanded Smart Distribution Networks. *IEEE Trans. Sustain. Energy* **2014**, *5*, 886–895. [[CrossRef](#)]
22. Delavari, A.; Kamwa, I. Improved Optimal Decentralized Load Modulation for Power System Primary Frequency Regulation. *IEEE Trans. Power Syst.* **2017**, *33*, 1013–1025. [[CrossRef](#)]
23. Shen, H.; Jiao, S.; Park, J.H.; Sreeram, V. An Improved Result on  $H_\infty$  Load Frequency Control for Power Systems with Time Delays. *IEEE Syst. J.* **2021**, *15*, 3238–3248. [[CrossRef](#)]
24. Carne, G.D.; Buticchi, G.; Liserre, M.; Vournas, C. Real-Time Primary Frequency Regulation Using Load Power Control by Smart Transformers. *IEEE Trans. Smart Grid* **2020**, *10*, 5630–5639. [[CrossRef](#)]
25. Rezkalla, M.; Zecchino, A.; Pertl, M.; Marinelli, M. Grid Frequency Support by Single-phase Electric Vehicles Employing an Innovative Virtual Inertia Controller. In Proceedings of the 2016 51st International Universities Power Engineering Conference (UPEC), Coimbra, Portugal, 6–9 September 2016; pp. 1–6.
26. Yao, Y.; Zhang, P.; Wang, Y. A two-layer control method for thermostatically controlled loads to provide fast frequency regulation. *Proc. CSEE* **2018**, *38*, 4987–4998.

**Disclaimer/Publisher's Note:** The statements, opinions and data contained in all publications are solely those of the individual author(s) and contributor(s) and not of MDPI and/or the editor(s). MDPI and/or the editor(s) disclaim responsibility for any injury to people or property resulting from any ideas, methods, instructions or products referred to in the content.